Theoretical study of the structure of lithium clusters

René Fournier, Joey Bo Yi Cheng, and Anna Wong
Department of Chemistry, York University, Toronto, Ontario M3J 1P3, Canada

(Received 29 January 2003; accepted 11 August 2003)

Lithium clusters Li_n ($n=5$ to 20) were studied by Kohn–Sham theory with local spin density and gradient-corrected energy functionals. We used a Tabu Search algorithm for structure optimization. The lowest energy Li_n isomers that we found fall in two categories: (i) the pentagonal bipyramid, icosahedron, and related structures which are typical of most pair potentials, and (ii) structures containing centered square antiprisms which are reminiscent of the bulk bcc structure and have two characteristic peaks in the pair distribution function, one near 2.60 Å and the other near 3.05 Å. Calculated isomer energies and vibrational frequencies suggest that, at room temperature, many cluster sizes should show liquidlike behavior or coexistence of multiple isomers. The number of unpaired electrons ''M'' as a function of cluster size ''n'' generally alternates between 0 (singlet) and 1 (doublet), but some cluster sizes display anomalous spin magnetic moments $M(n)$; they are $M(13)=5$, $M(16)=2$, $M(17)=3$, and $M(18)=2$. The Li_7, Li_8, Li_{19}, and Li_{20} clusters are particularly stable: they each have a very compact structure and a shape consistent with the ellipsoidal jellium model. © *2003 American Institute of Physics.* [DOI: 10.1063/1.1615237]

I. INTRODUCTION

The properties of small atomic clusters A_n vary as a function of n, with rather strong variations at small n (roughly $n<100$) and fairly smooth approach to bulk properties at larger n.[1] Small clusters can exhibit properties qualitatively different from the bulk.[2,3] The addition of a single atom to a cluster sometimes has dramatic effects on its reactivity.[4,5] We would like to explain these changes in cluster properties on the basis of electronic and geometric structure, but relatively little is known about that. Clusters of rare gases,[6–10] C,[11] Si,[12–14] Nb,[15] and other elements are quite different from fragments of crystalline solids. In some cases, cluster geometries are governed by simple principles and can be guessed fairly easily. For instance, fullerenes (C_n, $n \geqslant 60$) adopt cage structures where every atom is three-coordinated and no pentagonal ring shares an edge with another pentagonal ring,[11] and clusters of rare gas elements follow an icosahedral growth sequence that maximizes the number of nearest neighbors.[8,9] There is experimental evidence for icosahedral structure for Ni (Ref. 16) and Al (Ref. 17) clusters, and some of the larger Cu (Ref. 18) and Co (Refs. 19 and 20) clusters. But the principles that govern the structure of clusters of most elements are not fully understood. As a result, it is quite difficult to guess cluster structure and make sense of measured properties and chemical reactivities.[5]

Lithium looks like a good starting point for a theoretical understanding of metal clusters because Li is the lightest metallic element and it has a single *s* valence electron. The jellium model accounts nicely for the relative stability of *s*-only valence metal clusters,[21,22] so it could help explain properties of Li clusters. But previous theoretical work shows that Li clusters are not so simple: some have unusual spin states or structure,[23,24] others are fluxional and display a complicated dynamics.[25–27] Recent experiments[28] and calculations[29] on Li_4^- show a complex interplay between geometry, electronic structure, and spin multiplicity.

The huge number of possible isomers generally makes theoretical studies of cluster structure very complicated. The number of distinct minima on a model Lennard-Jones potential energy surface grows exponentially with n, and at $n=13$ it is already more than 1000.[9] We expect roughly the same for metallic elements. The huge number of isomers is not so problematic if one or few isomers have a much lower energy than the rest *and* structural principles help discover those few isomers. But metal clusters are held together by many weak bonds, so multiple low-energy isomers are likely, and although there are some guiding ideas about metal cluster structure,[30–32] there is no simple set of rules as for, say, fullerenes. Therefore, it is important to make an extensive search of possible low-energy cluster isomers. We have devised a global optimization algorithm, which we call ''Tabu Search in Descriptor Space'' (TSDS), specifically for searching low-energy cluster isomers on potential surfaces calculated by *first principles*.[33] We used a TSDS for the present study. Details of the TSDS method are given elsewhere,[33] but we will give a brief outline in the next section.

Previous studies have looked at many different aspects of lithium clusters: factors affecting the structures of Li_n and other alkali metal clusters,[30] the structure of Li_n,[23,24,34] their optical absorption spectra,[35–38] fluxional Li_5,[25] fluxional Li_8 and Li_{20},[26,27] dynamics of Li_8,[39] ionization potential and electron affinities of Li_n ($n=2,4,6,8$),[40–42] and shell effects on the fission of cluster dications.[43,44]

Gardet *et al.*[24] studied structure using a PBP growth sequence model for clusters with up to 20 atoms, and examined the effect of exchange-correlation functional on relative isomer energies. Sung *et al.*[23] did an *ab initio* molecular dynamics global search for minima of Li_n for $n=3-25$ and a few larger clusters. They discovered unusual ''solvated ion''

structures characterized by the presence of centered trigonal prisms (CTP) units and a mix of short and long bonds. Rousseau and Marx analyzed the nature of bonding in lithium clusters and bulk using the ''electron localization function.'' [45] They discussed the $p\pi$ interactions and multicenter bonding and how they affect the geometrical structure.

In this article we describe a systematic unbiased search for low energy isomers of Li clusters with up to 20 atoms. The energy was calculated by Kohn–Sham theory with two different exchange-correlation functionals. In one set of calculations we used a very large basis set. We report the structure of low energy isomers, their energies, ionization potentials, and vibrational frequencies.

II. COMPUTATIONAL DETAILS

A. Calculation of total energy

We used Kohn–Sham density functional theory (KS-DFT) and the program deMonKS3p2[46] and did three series of calculations with different treatments of exchange-correlation (XC) and basis sets.

For XC, we used the local spin density (LSD) functional of Vosko, Wilk, and Nusair[47] (VWN), and a gradient-corrected functional that combines the corrections of Becke for exchange[48] and Perdew for correlation[49] (BP86 functional). The basis sets were a ''DZVP'' basis with three *s*-type, one *p*-type, and one *d*-type functions and a (721/1/1) contracted Gaussian pattern, and a very large basis (''cc-pV5Z'') consisting of six *s*-type, five *p*-type, and four *d*-type contracted Gaussian functions. The three combinations of XC and basis sets that we used would normally be denoted by VWN/cc-pV5Z, VWN/DZVP, and BP86/DVZP, but instead we will use the shorter symbols ''LB,'' ''LS,'' and ''GS,'' respectively: *L* stands for ''local,'' *G* for ''gradient-corrected,'' *B* for ''big basis,'' and *S* for ''small basis.'' The big basis set was obtained from Feller's cc-pV5Z basis for Li,[50] which is related to Dunning's correlation consistent basis sets,[51] by deleting the *f*-, *g*-, and *h*-type functions. We decided to use such a large basis because Sung *et al.* had found some remarkable energy minima with one or few Li ions solvated (surrounded) by several Li atoms carrying partial charges. These isomers have a mix of atoms with high (eight or more) and low (five or lower) coordination,[23] a mix of short and long bonds, and large ionic character. A flexible basis is needed to describe atomic environments that are so different, and our calculations indeed show that the energy of solvated ion isomers, relative to that of other structures, change significantly with basis set.

The best of the three methods is clearly LB; it gives accurate results for Li_2 (see Table I) and a very good extrapolated bulk cohesive energy (see Sec. IV). But there are few data to compare with for clusters and, in principle, combining gradient corrections with the large basis set (method GB) might be better. We did four test calculations using GB (see subsections on 13- and 14-atom clusters) and find relative energies that are close to what one would estimate assuming additivity of basis set and exchange-correlation effects on energies, i.e., $E(\mathrm{GB}) \approx E(\mathrm{LB}) + E(\mathrm{GS}) - E(\mathrm{LS})$.

The grid for numerical evaluation of the XC energy had 64 radial shells of points, and each shell had 50, 110, or 194 angular points depending on the distance to the nucleus (''FINE'' option in deMon). After a global optimization sequence, selected geometries were optimized by a quasi-Newton method until the norm of the gradient was typically 5×10^{-5} atomic units (au) or less.

TABLE I. Spectroscopic parameters for Li_2, with DZVP basis set in all cases except the first VWN calculation.

	D_0^0 (eV)	R_e (Å)	ω_e (cm^{-1})
Expt. (Ref. 56)	1.05	2.6729	351
VWN/cc-pV5Z	1.024	2.714	335
VWN	0.94	2.763	328
PVS	0.51	2.744	331
BP86	0.81	2.770	325
BPVS	0.86	2.770	321
BLAP	0.64	2.835	312
PW91	0.85	2.753	332

Table I shows results of our calculations on Li_2 using the DZVP basis set along with the VWN, BP86, and other[52] XC functionals. The Li_2 molecule is a rare case where LSD underestimates the experimental bond energy (0.94 vs 1.05 eV) and overestimates the bond length (2.76 vs 2.6729 Å). Other functionals are better in principle, but they give even smaller binding energies, and little or no improvement on the bond length. Hybrid functionals such as B3LYP do not look like a good choice for metal clusters because of the known deficiencies in Hartree–Fock theory for metals and other theoretical arguments against them.[53] Further, hybrid functionals are fitted to databases of molecules containing very few metal–metal bonds and they are not particularly good for transition metal dimers.[54,55]

B. Global minimum search

Global optimization of clusters normally requires very many energy evaluations, thousands or more typically. The computational cost involved precludes the use of first-principles methods such as Kohn–Sham density functional theory (KS-DFT). We devised a TSDS method that requires very few energy evaluations (only a few hundreds), yet does a reasonably good search of the global minimum. Of course, a search with few function evaluations cannot *generally* be as good as a search, by a different algorithm, with many more function evaluations.

In the TSDS method, we seek a compromise that greatly speeds up the search at the cost of requiring ''expert input.'' The user must supply information to the algorithm in the form of definitions of structural descriptors. The TSDS evaluates the numerical values of these descriptors, and the energy, for a set of initial structures. Then, it generates thousands of candidate structures by modifying structures for which the energy has already been evaluated. The TSDS assumes a correlation between energy and descriptors and calculates an estimate of the energy for each of the candidate structures by interpolation in descriptor space. Next, the TSDS assigns a score to candidate structures on the basis of three criteria: (i) the estimated energy (lower energies are better), (ii) the similarity between a candidate's descriptors

and those of all previous structures (less similar is better), and (iii) a random variable. The first criterion puts a bias toward searching more thoroughly in low-energy regions, the second one tends to drive the search into new regions of configuration space, and the third one allows to visit or revisit any structure, albeit with small probability if the first two criteria are unfavorable. The TSDS sorts candidate structures by their score and keeps only a few (typically 10) out of many (typically 1000) structures. It calculates the KS-DFT energy only for those few, and updates the dataset of structures with known energy. This cycle is repeated many times.

A potential drawback of TSDS is the danger of overlooking stable structures if they are atypical. As a TSDS search progresses, it gradually excludes entire regions of configuration space. If two clusters have similar descriptors but very different energies, one being the global minimum and the other being a high energy structure, and the TSDS visits the high-energy structure first, it will tend to avoid any further search in that region of descriptor space. If this happens, it is unlikely for TSDS to find the global minimum, even with many more energy evaluations. But this is hardly a problem when computational cost strictly limits the number of function evaluations anyway. Of course, if structural descriptors do correlate with energy, the risk that the TSDS excludes the global minimum is quite small. That is why the choice of descriptors is important.

Here are three of the seven descriptors that we used for optimization. The mean coordination c is defined as

$$c=(1/n)\sum_{i=1}^{n} c_i=(1/n)\sum_{i=1}^{n}\sum_{j\neq i} f(R_{ij};R_c), \tag{1}$$

where R_{ij} is the distance between atoms i and j, R_c is a cutoff distance which we set equal to 1.2 times the bulk nearest-neighbor distance, and $f(R_{ij};R_c)$ equals 1 if $R_{ij}<R_c$ and equals 0 otherwise. A better definition is to take a differentiable cutoff function instead, but this kind of detail has little effect on a TSDS optimization. Two other descriptors, the asphericity ζ and shape η, seem important for metal clusters:

$$\zeta=\frac{(I_a-I_b)^2+(I_b-I_c)^2+(I_c-I_a)^2}{I_a^2+I_b^2+I_c^2}, \tag{2}$$

$$\eta=(2I_b-I_a-I_c)/I_a\,. \tag{3}$$

Here, $I_a\geqslant I_b\geqslant I_c$ are the three moments of inertia of the cluster. The larger ζ is, the further from spherical a structure is. Positive values of η correspond to prolate structures and negative values correspond to oblate structures. The ellipsoidal jellium model (EJM) makes simple predictions about the optimal shape of metal clusters based on the number of delocalized electrons N_e.[21,22] In particular, it predicts spherical shapes for clusters with $N_e=8$, 19, and 20, prolate shapes for $N_e=9-13$, and oblate shapes for $N_e=14-18$.

During the study, we found that the number of interior atoms might be an important aspect of structure. We did not use it in the TSDS optimization, but we did use it for analyzing the final results. There is no clear cut way of deciding if an atom is an ''interior atom'' or a ''surface atom,'' but we define the number I of interior atoms in a clusters as follows:

$$\begin{aligned} &f_{ij}=(R_{ij})^{-6},\\ &\vec{v}_i=\sum_{j\neq i} f_{ij}[(\vec{R}_i-\vec{R}_j)/R_{ij}]\Big/\sum_{j\neq i} f_{ij},\\ &s_i=(1-|\vec{v}_i|)^6,\\ &I=\sum_i s_i\,. \end{aligned} \tag{4}$$

In these equations f_{ij} is a rapidly decreasing function of R_{ij} chosen arbitrarily, and $\vec{v}_i$ is a weighted sum of unit vectors between atom i and all other atoms (only the nearest neighbors of i contribute appreciably because of the factor f_{ij}). The norm of $\vec{v}_i$ is very small if atoms are distributed isotropically around atom i. We chose the power 6 in the definition of s_i to create a sharp distinction between interior atoms (with $s_i\approx 1$) and other atoms ($s_i\approx 0$). Then, I gives an objective measure for the number of interior atoms in a cluster.

Here is an illustration of how TSDS works. When TSDS searches the global minimum of Li_{20}, it quickly ''learns'' that every structure with $c<5$ or $\eta>0.3$ has a very high energy, so it stops searching regions of configuration space where structures are elongated or atoms have low coordination. Nothing prevents the TSDS to generate such structures *a priori*, but the probability of visiting them becomes small after structures with similar descriptors have been found to have very high energies.

We did the TSDS global optimization with the LB method to make sure that we do not rule out any unusual structure that would not be described adequately by a small basis set. Then we did local optimization on the best structures found by TSDS with each of the three methods, LB, LS, and GS. After that, we generated a few additional structures by modifying the best structures that had been found. This yielded slightly lower energy minima in some cases. This shows that our TSDS search was incomplete and our final results may not include the global minimum, especially for $n\geqslant 18$. This is always a problem in global optimization. We note, however, that we found lower energy isomers than reported in previous studies at many cluster sizes, including clusters with triplet or higher spin states never reported before at sizes $n=16-18$.

C. Local optimization

Following the TSDS, we sorted clusters with a combination of two criteria: the LB energy and how similar descriptors are to those of lower energy clusters. The second criterion gives low priority to structures that are similar to lower-energy ones in order to avoid doing several local optimizations that yield the same structure. We used that second criterion conservatively, and, as a result, we had many instances of separate local optimization runs leading to the same minimum. We did a quasi-Newton local optimization for the first few (typically ten) structures in the order in which clusters were sorted. Local optimization yields an extremum but not always a minimum. The eigenvalues of the energy second derivatives matrix are needed to decide whether a stationary point on the potential surface is a minimum. We did this calculation by finite difference of gradients

TABLE II. Acronym, name, number of atoms, and ideal symmetry point group of key cluster structures.

CSAP: centered square antiprism	9	D_{4d}
CTP: centered trigonal prism	7	D_{3h}
DCSAP: double CSAP	14	D_{4h}
DD: dodecahedron	8	D_{2d}
DICO: double icosahedron	19	D_{5h}
DICO-1: DICO with a missing atom	18	C_{5v}
DTCTP: double TCTP	17	D_{3h}
ICO: icosahedron	13	I_h
PBP: pentagonal bipyramid	7	D_{5h}
TCTP: tricapped CTP	10	D_{3h}
TT: tetracapped tetrahedron	8	T_d

for the most stable structures of each cluster size in the VWN/DZVP approximation only. The lowest frequencies are the most difficult to calculate accurately, so they should be taken with caution. But they are also the most interesting because they give a simple way of characterizing clusters as ''quasi-rigid'' or ''nonrigid.'' Our normal mode analysis program does not eliminate rotation and translation modes. Because of numerical errors, the six smallest frequencies are not exactly zero, but they are almost always within ± 10 cm^{-1} of zero. The negative frequencies reported here actually are imaginary frequencies. We say a structure is a minimum when its six lowest frequencies are in the interval from -10 to $+10$ cm^{-1}. One of the column in Table I shows the lowest frequency *not* in the interval $[-10, +10]$ cm^{-1} for a given structure. When that frequency is positive it indicates a minimum and when it is negative (imaginary) it indicates a transition state; when its absolute value is smaller than 20 cm^{-1}, the potential surface is very flat and the nature of the critical point (minimum or transition state) is in doubt. For example, the isomer 12.3 (Table III) has a value of 15 cm^{-1}, but the six lowest calculated frequencies vary between -6 and $+6$ cm^{-1} when they should really all be zero, therefore the calculated 15 cm^{-1} is barely larger than the numerical uncertainty.

III. CLUSTER ISOMERS

We obtained similar isomers by the LB, LS, and GS methods; in most cases the minimum of one method is well approximated by uniformly scaling the coordinates of another. Normal mode analysis was done only with LS. Unless stated otherwise, our discussion applies to LB energies and structures, and LS vibrational frequencies and HOMO-LUMO gaps. There are some cases with significant differences between LB and either LS or GS results and we will point them out. Acronyms that we use for high-symmetry structures of special importance are summarized in Table II. We use the general notation $n.m$ to label isomers, where n is the number of atoms, and m is the rank by energy among the structures we found.[57] Most Li_n optimized structures fall in one of two categories: structures derived from the 7-atom PBP or 13-atom ICO, and structures derived from the 9-atom CSAP or 10-atom TCTP (the Li_{16} global minimum of Fig. 1 falls in that category). Multiple CSAP and TCTP units allow more compact structures than do the PBP and ICO, but they require a combination of short and long bonds. Apparently, CSAP structures do not show up in clusters of late transition metals which have fcc crystal structure. On the other hand, the bcc crystal structure has every atom in a local environment similar to that of the central atom in the CSAP. We surmise that the relative stability of PBP and CSAP cluster structures correlates with the relative stability of the fcc and bcc crystal structures.

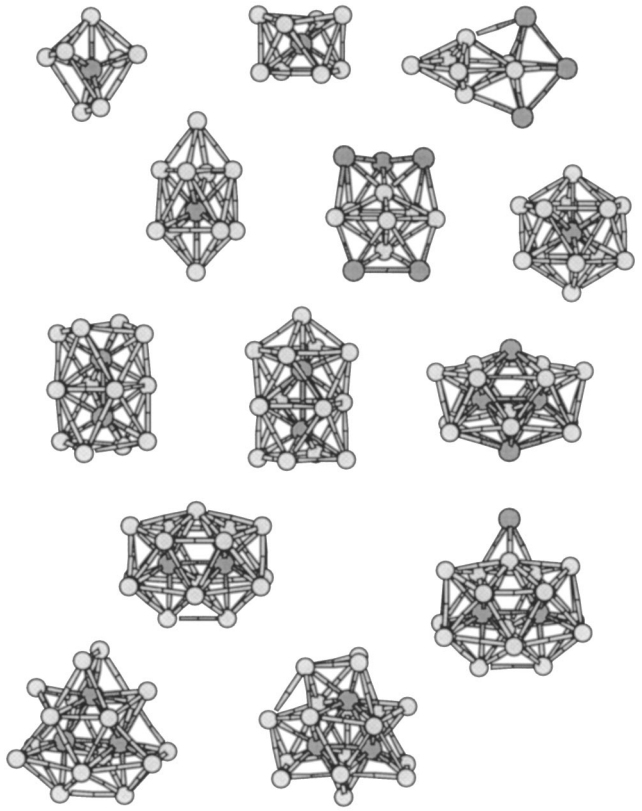

FIG. 1. Lowest energy isomers of Li_n clusters ($n=8-20$) obtained by LB calculations.

Some atoms are given a darker shade in Fig. 1. They are (i) the interior atoms of Li_8, Li_9, Li_{11}, $Li_{13}-Li_{20}$; (ii) the atoms that make up a rhombus unit in Li_{16}; (iii) atoms capping a PBP in Li_{10} and Li_{12}, and (iv) the capping atom of Li_{18} relative to Li_{17}.

A. Lowest energy isomers

Discrepancies occur in relative energies calculated by different methods for certain isomers. In some cases, the minimum of one calculation relaxes to a different minimum in another calculation, so it is not always possible to make direct comparisons between methods. But there are many cases where direct comparison is possible, and where one finds genuine differences between calculated energies. The most important of these cases are the 9-atom bicapped PBP 9.3 relative to the CSAP 9.1; the 13-atom tetracapped CSAP 13.2 relative to sextet ICO 13.1; the 14-atom capped ICO relative to 14.2 (a low symmetry multiply capped PBP); and the 15-atom bicapped ICO 15.2 relative to the capped DCSAP 15.1. As a rule, high spin states tend to be relatively more stable in LB calculations. Another trend is that CSAP

TABLE III. Smallest LS harmonic frequency (cm^{-1}), HOMO-LUMO gap (LS, in eV), and relative energies (eV) for different Li_n structures, $n=8-12$. The number of unpaired electrons, M, is shown when it is neither 0 or 1.

	ω_{min}	Gap	LB	LS	GS
8.1 C_{2v}		1.36	0.00	0.04	0.08
8.2		0.81	0.04	0.01	0.03
8.3		1.25	0.09	0.00	0.00
8.4		0.73	0.10	0.00	0.04
9.1 C_s	25	0.23	0.00	0.01	0.03
9.2	59	0.23	0.01	0.00	0.00
9.3	70	0.50	0.19	0.04	0.03
10.1 D_{2d}	70	0.78	0.00	0.00	0.00
11.1 C_s	81	0.24	0.00	0.06	0.07
11.2 $M=3$	91	0.43	0.04	0.12	0.07
11.3	60	0.59	0.07	0.00	0.00
12.1 C_s	58	0.55	0.00	0.00	0.00
12.2	−42	0.42	0.07	0.15	0.18
12.3	15	0.46	0.10	0.11	0.12

TABLE IV. Smallest VWN/DZVP harmonic frequency (cm^{-1}), HOMO-LUMO gap (VWN/DZVP, in eV), and relative energies (eV) for different Li_n structures, $n=13-16$. The number of unpaired electrons, M, is shown when it is neither 0 or 1.

	ω_{min}	Gap	LB	LS	GS
13.1 I_h, $M=5$	147	0.32	0.00	0.02	0.00
13.2	71	0.40	0.05	0.00	0.11
13.3	52	0.40	0.10	0.03	0.13
13.4	72	0.52	0.12	0.00	0.10
13.5	75	0.40	0.12	0.02	0.12
14.1 D_{2h}	46	0.73	0.00	0.00	0.02
14.2	71	0.81	0.07	0.01	0.00
15.1 C_{2v}	57	0.25	0.00	0.00	0.00
15.2, $M=3$	74	0.20	0.18	0.15	0.03
16.1 C_{2v}, $M=2$	64	0.42	0.00	0.00	0.00
16.2	47	0.26	0.23	0.16	0.10

and CTP structures get stabilized relative to PBP and ICO structures as we go from small to large basis set.

We must stress that even our best estimates of relative energies (LB) have limitations, mainly for two reasons. First, better theoretical treatments are possible and they would yield somewhat different relative energies. Since energy differences between lithium cluster isomers are small, the energy ordering of the isomers could change. Second, a more meaningful connection to experiment can be made by calculating *free energies*. We ignored the entropic term because of uncertainties in our calculated low-frequency modes and in the validity of the harmonic approximation for lithium clusters. However, we estimated the vibrational and electronic contributions to $T\Delta S$ (at 298 K) with a standard formula[58] and our calculated frequencies and ground state degeneracies for several isomers. Ignoring cases where there is a calculated frequency below 20 cm^{-1}, we find that $T\Delta S$ (298 K) typically varies over a range of 0.05 eV between different isomers of a given size.

Relative energies normally agree to within roughly 0.1 eV between the different methods (see Tables III, IV, and V), or they are large enough to rule out the structure. The method we trust most for relative energies is LB, because it gives good results for Li_2 and good extrapolated bulk cohesive energy. But LB relative isomer energies must have uncertainties of at least 0.1 eV. With that in mind, it seems very likely that many Li_n isomers will coexist at room temperature at sizes $n=9$, 11, 13, 14, 18, 20. Ruling out the possibility of multiple isomers is harder. For that we would need relative energies in excess of 0.1 eV *and* be confident that our search for minima was sufficiently thorough, but it is not possible to guarantee that. Still, our results suggest that room temperature Li clusters may consist of a single isomer at sizes $n=10$, 15, and 16. In the remainder of this section we will make brief comments for each cluster size.

Li_8—The smallest solvated ion isomer found by Sung *et al.* is a capped CTP Li_8. That isomer (8.1) is the global minimum in our large basis set calculation, but three other isomers are quite close in energy, a C_s symmetry capped PBP (8.2), a TT (8.3), and a DD (8.4). Smaller basis sets destabilize the capped CTP relative to the other three. The capped CTP can be viewed as a bicapped octahedron where the atom with highest coordination moves toward the center of mass of the cluster and the two capping atoms move within bonding distance of each other. Reichardt *et al.*[39] did BLYP calculations and obtained a minimum similar to 8.1, except it has a C_{3v} symmetry point group. Their molecular dynamics simulations showed that this isomer interconverts easily with the C_s capped PBP. The potential surface appears very flat in the region of configuration space containing structures with one 7-coordinated atom: details in basis set and treatment of exchange-correlation can probably bring qualitative changes in the isomers one finds.

Li_9—There are many CSAP structures corresponding to different ways of lowering the ideal D_{4d} symmetry, all within a very small energy range. We show only the lowest energy one (9.1) in Table III. Some of these appear to be minima, others transition states, but our calculations are not accurate enough to distinguish between these possibilities. The potential energy surface is too flat given our numerical approximations (finite basis and grid, imperfect convergence

TABLE V. Smallest LS harmonic frequency (cm^{-1}), HOMO-LUMO gap (LS, in eV), and relative energies (eV) for different Li_n structures, $n=17-20$. The number of unpaired electrons, M, is shown when it is neither 0 or 1.

	ω_{min}	Gap	LB	LS	GS
17.1 D_{3h}, $M=3$	84	0.61	0.00	0.00	0.00
17.2, $M=3$	20	0.54	0.12	0.09	0.09
18.1 C_s, $M=2$	13	0.18	0.00	0.01	0.00
18.2	63	0.23	0.05	0.00	0.08
19.1 C_{2v}	46	0.61	0.00	0.00	0.00
19.2	17	0.59	0.11	0.09	0.12
20.1 C_s	19	1.05	0.00	0.00	0.00
20.2	44	0.68	0.11	0.02	0.00

of SCF and geometries, etc.). The smallest frequency in 9.1 (a CSAP), 9.2 (a tetracapped TBP), and 9.3 (a bicapped PBP) shows that they are minima. Isomer 9.3 relaxes to 9.1 in LB but it is a distinct minimum in the other two calculations. One can go from 9.3 to 9.2 and then 9.1 with rather small atomic displacements. The high symmetry D_{4d} CSAP could serve as a branching point between isomers of a fluxional Li_9. It seems very likely that Li_9 is fluxional at room temperature, but a dynamics study with a very accurate potential energy would be desirable to investigate this.

Li_{10}—The situation is different for Li_{10}. All three sets of calculations find the D_{2d} isomer 10.1 (a triply capped PBP) more stable than the next isomer (a capped CSAP) by 0.1 eV. It is likely that one isomer dominates Li_{10} at room temperature.

Li_{11}—There seems to be three energy minima with very different characteristics in a 0.1 eV energy range: a D_{4d} CSAP capped on both ends (11.2) with quartet ground state (shown as $M=3$ in Table III), a similar bicapped CSAP but with C_s symmetry and doublet spin state (11.1), and a tetracapped PBP doublet (11.3, the same structure we found for Ag_{11}). Apparently, the CSAP Li_9 and doubly capped CSAP Li_{11} have not been considered before in first-principles studies of Li clusters. The lowest energy minimum of Li_{11} is the fourfold equivalent of an icosahedron. It is the first in a series of structures with capped CSAP units that generally have more interior atoms than clusters of the PBP and ICO growth sequence. We discuss factors that may explain the stability of CSAP structures in Sec. III B.

Li_{12}—Our global minimum is a PBP with five capping atoms; it is the same structure that we found for Ag_{12}.[59] The next two most stable isomers (0.07 and 0.10 eV higher) are multiply capped CSAP. We also found two multiply capped PBP 0.16 and 0.21 eV above 12.1.

Li_{13}—There are many low-energy minima for Li_{13} with very different characteristics: an icosahedron, several multiply capped PBP, and two C_s symmetry CSAP derived structures. The BP86 calculations predict the sextet ICO to be 0.11 eV more stable than any other isomer, but our preferred method predicts a CSAP structure (11.1 with two capping atoms) is only 0.05 eV higher. It seems quite likely that experiments would see a mixture of isomers. The ICO had been found by Gardet *et al.*[24] It is remarkable in many ways: it has a high symmetry (I_h), an unusual high spin magnetic moment (five unpaired electrons in a degenerate orbital), and the large value of its lowest vibrational frequency (147 cm^{-1}) indicates it is comparatively rigid. We did additional calculations for 13.1 and 13.2 with gradient corrections and the big basis set. With this ''GB'' method, 13.1 is the most stable and 13.2 is 0.175 eV higher.

Li_{14}—Two low-energy structures are predicted, a prolate DCSAP distorted from the ideal D_{4h} symmetry point group to D_{2h}, and an oblate multiply capped PBP with C_2 symmetry (14.2). The TSDS rediscovered the latter several times despite the built-in tendency of TSDS to steer away from previously discovered minima. We were concerned that the TSDS may have missed important structures and so we tried others. A T_d structure can be made by adding six symmetry equivalent capping atoms to the T_d tetracapped tetrahedron. We find it 1.16 eV higher than 14.2. Sung *et al.* reported a tetracapped double centered trigonal prism depicted in Fig. 2(c) of Ref. 23 as their global minimum. Viewed under a different angle, this structure looks like a DCSAP. We tried two distorted DCSAP structures. Compared to 14.2, one of them is roughly 0.5 eV less stable, and the other is 0.07 eV *more* stable so it is our tentative global minimum. The next most stable isomer is the capped ICO at +0.26 eV. The stability of 14.2 is a bit surprising. The DCSAP and capped ICO each have 45 formal bonds (45 pairs of atoms within the distance cutoff) and high symmetry. By contrast, 14.2 has only 42 bonds and it has low symmetry. We think that the stability of 14.2 is explained by its oblate shape (the shape parameter is −0.37) on the basis of the EJM.[21] The stability of DCSAP, despite a strongly prolate shape, shows the propensity of Li_n for having interior atoms. As for Li_{13}, we did GB calculations for 14.1 and 14.2: these two isomers are almost degenerate according to GB, with 14.2 only 0.007 eV higher than 14.1.

Li_{15}—The 15.1 isomer is a double CSAP (two CSAP sharing a square face) plus a top capping atom formally with C_{4v} symmetry but distorted to C_{2v}. This capped DCSAP seems to have two interior atoms, one for each CSAP, but it has $I=1.57$ (Table VI). The average of the 13 distances between interior and ''surface'' atoms is 2.71 Å, the average distance between surface atoms is 3.22 Å, and the distance between the two interior atoms is 2.97 Å, intermediate between 2.71 and 3.22. The ratio of 3.22 and 2.71, 1.19, is close to that for bcc first and second neighbors ($2/\sqrt{3}=1.15$).

Li_{16}—The global minimum has a triplet ground state. It can be obtained by distorting a triply capped ICO which is 16.2, our second lowest energy isomer 0.23 eV above 16.1. However, using a smaller basis set and gradient corrected functional decreases the energy separation between 16.1 and 16.2: it becomes 0.16 and 0.10 eV, respectively. Still, we suggest that only 16.1 should be observed in experiments. The distortion from 16.2 to 16.1 has practically no effect on the descriptors c, ζ, and η, and very little effect on the HOMO-LUMO gap, but it increases I from 1.04 to 1.94. Another effect of the distortion is to increase the smallest atomic coordination from 4 to 5, and to decrease the largest atomic coordination from 12 to 10. The Li_{16} global minimum is remarkable because of its stability, and because it has two interior atoms: in the PBP growth sequence, it is only at $n=19$, with the double icosahedron (DICO), that a second interior atom appears. Furthermore, the most stable isomers that we found for $n=15$ and 17–20 are all related to 16.1 as should be clear from Fig. 1. The 16.1 isomer and related structures will probably be less stable in elements where the ratio of the size of valence and core orbitals is smaller, such as late transition metals.

Since CSAP structures are generally favorable, we tried the D_{4h} doubly (top and bottom) capped double CSAP. It can be viewed as the fourfold equivalent to the double icosahedron (DICO). Its LS relative energy is very high, 0.30 eV, although it is as compact a structure (descriptor $c=6.72$) as 16.1 ($c=6.66$) and it is more symmetrical. We think that the doubly capped DCSAP is unstable because its shape (ζ

TABLE VI. Shape descriptors of the lowest energy isomers.

	$\bar{c}$	ζ	η	I
8.1	4.36	0.01	−0.10	0.62
8.2	4.75	0.07	−0.05	0.12
8.3	4.50	0.00	0.00	0.03
8.4	4.90	0.07	0.20	0.31
9.1	5.11	0.07	−0.16	0.14
9.3	4.89	0.06	0.24	0.04
10.1	5.20	0.22	0.50	0.05
10.2	5.24	0.20	0.47	0.71
11.1	5.90	0.13	0.25	0.87
11.2	6.16	0.07	0.29	1.00
11.3	5.45	0.28	0.23	0.10
12.1	5.67	0.24	0.14	0.19
12.2	5.73	0.15	0.23	0.92
13.1	6.46	0.00	0.00	1.01
13.2	6.11	0.19	0.37	0.83
13.3	5.87	0.16	0.19	0.81
13.4	5.85	0.18	−0.03	0.20
13.5	5.85	0.18	−0.07	0.18
14.1	5.96	0.14	0.34	1.98
14.2	6.00	0.17	−0.37	0.21
14.3	6.43	0.06	0.27	0.88
15.1	6.43	0.14	0.33	1.57
15.2	6.53	0.09	0.19	0.89
16.1	6.66	0.08	0.16	1.94
16.4	6.72	0.23	0.46	1.91
17.1	6.98	0.07	0.30	1.99
17.3	6.71	0.05	0.26	1.10
18.1	6.90	0.04	−0.06	1.99
18.1 ($M=2$)	6.86	0.05	−0.11	1.94
18.2	6.89	0.04	0.22	1.36
19.1	6.92	0.02	−0.16	2.11
19.2	7.02	0.03	0.11	2.03
20.1	6.84	0.00	−0.02	2.01
20.2	7.00	0.00	−0.01	1.69
20.3	6.90	0.00	0.03	1.68

$=0.23, \eta=0.46$) is much further from the EJM ideal shape (oblate) than 16.1 is ($\zeta=0.08, \eta=0.16$). The HOMO-LUMO gaps are in line with this idea, quite small for the doubly capped CSAP (0.19 eV), larger for 16.1 (0.42 eV).

Li_{17}—There is a close relation between the 17-atom global minimum, a D_{3h} double tricapped centered trigonal prism (DTCTP, 17.1), and 16.1, although the latter has no obvious trigonal prism motif. Putting 17.1 in an orientation where the threefold axis is along *z*, one can replace a pair of symmetry equivalent capping atoms related by reflection in the horizontal plane by a single atom at the average of their positions. Then, a 16.1 structure is obtained by relaxation of the nearest neighbors to that atom. The most remarkable feature of 17.1 and 16.1 is that they have achieved two interior atoms (their *I* descriptors are 1.99 and 1.94, respectively) at a smaller nuclearity than the icosahedral growth does (19).

Li_{18}—We find two low energy structures, one of CSAP type, and the other a DICO-1 (PBP type). The CSAP structure (18.1) has a triplet ground state; the corresponding singlet is only 0.05 eV higher. The C_{5v} symmetry DICO-1 (18.2) is 0.05 eV above 18.1, it has a singlet ground state, and the triplet DICO-1 is 0.07 eV further up in energy. The small energy differences suggest that several isomers and spin states could be present in experiments.

Li_{19}—A bicapped DTCTP with C_{2v} symmetry[60] is our tentative global minimum (19.1). A multiply capped ICO is 0.11 eV higher. The double icosahedron (DICO) ($M=5$ ground state) is much higher in energy, approximately 0.66 eV above 19.1. The BP86 functional stabilizes the high symmetry and high spin 13-atom ICO by approximately 0.1 eV relative to VWN. This kind of energy shift is not enough to bring the sextet DICO close in energy to 19.1.

Li_{20}—LB calculations predict a CSAP related structure as the most stable, 0.11 eV lower than any other. On inspection, it appears to have three interior atoms, but its descriptor *I* is 2.01. The smaller basis calculations yield the same global minimum but give at least four other structures, all of the PBP family, within 0.1 eV. The most remarkable thing about these isomers is that they all have asphericity (ζ) and shape (η) descriptors quite close to zero, in agreement with the prediction of the EJM for a 20-electron metal cluster.[21,22] Koutecký *et al.*[30] considered two high-symmetry quasispherical ($\zeta=\eta=0$) structures: a T_d fragment of the fcc crystal ("fcc") and a compact T_d structure they call SS (see their Fig. 5). We did a test calculation on the fcc structure and found it to be 2.16 eV above our global minimum. Koutecký *et al.* found the SS structure to be 0.78 eV more stable than fcc, which makes it roughly 1.4 eV less stable than our global minimum. Our TSDS optimization discovered several isomers that are more stable than that. This shows how difficult it is to obtain low energy cluster isomers without global optimization.

B. Structural trends

As noted before, structures generally fall in either the PBP or CSAP category. For transition metals, there is evidence that small clusters adopt PBP-type structures[59] and larger clusters have icosahedral structures[16–20] related to the PBP. The CSAP-type structures have not been discussed much before, but were mentioned in at least one earlier study of lithium clusters.[23] In our calculations PBP and CSAP structures have practically equal energies at nuclearity $n=11-14$ and 18, a PBP structure is favored at $n=10$, and CSAP structures seem favored at all other $n>8$. The CSAP itself is like a 9-atom fragment of the bcc crystal but with staggered square faces and small distortions. We view CSAP structures as rough cluster equivalents to the bulk bcc structure, therefore we do not expect PBP type Li_n clusters for $n>20$.

An essential difference between PBP and CSAP structures is shown in Fig. 2. Distribution functions of interatomic distances were obtained by replacing each bond length by a narrow (0.10 Å full width at half maximum) Gaussian distribution and summing over all atom pairs. They are shown for the computed global minima of Li_{10}, Li_{11}, and Li_{16}, and a low-lying isomer of Li_{14} (14.2, multiply capped PBP). The

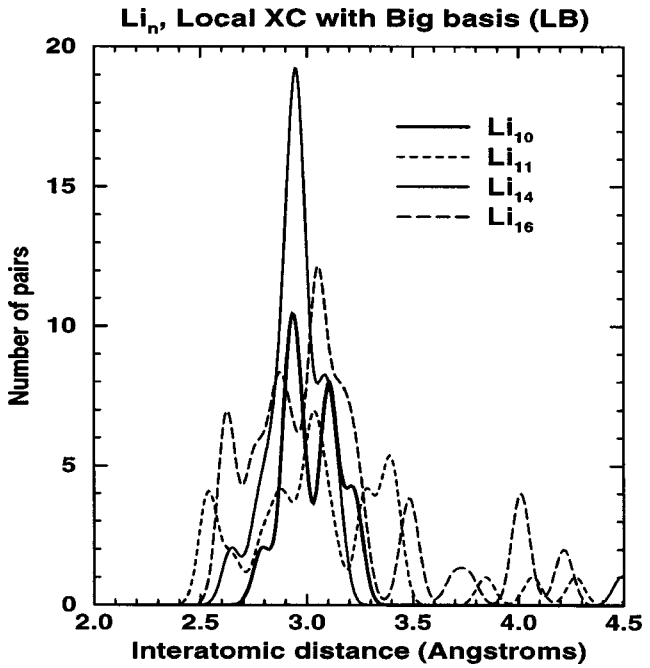

FIG. 2. Distribution of interatomic distances in Li_{10}, Li_{11}, Li_{14}, and Li_{16}.

Li_{10} and Li_{14} cases (shown as full lines) are representative of PBP structures, and Li_{11} and Li_{16} (dashed lines) are representative of CSAP structures. The PBP structures have a prominent peak near 2.95 Å, with smaller peaks or shoulders within 0.3 Å on either side of it, and essentially nothing else up to 4.5 Å. Clusters of CSAP type have a broader and more complicated distribution. It extends to very short distances (roughly 2.5 Å), and it has characteristic peaks near 2.60 and 3.05 Å and additional peaks in between and at larger distances (3.3 to 4.4 Å).

Doye, Wales, and Berry discussed the implications of interatomic potential range on cluster structure and relative stability of liquids and solids.[61] Their line of reasoning helps contrast the structures that we found for Li and Ag clusters.[59] Lithium can accomodate the mix of short and long bonds necessary for CSAP structures and for the bulk bcc crystal structure, because it has a long-ranged interaction potential, i.e., the force constant in Li_2 is small. This can be understood by considering the radius of the core (R_c) and of the *s*-valence orbital (R_v) of lithium: R_c is much smaller than R_v, so the potential energy does not increase too steeply when Li–Li bonds are compressed, and this is favorable for the formation of CSAP and bcc structures. The same holds true for other alkali, but maybe not to the same extent, so CSAP structures are not necessarily favored in other alkali clusters. In late transition metals the core is comparatively big, therefore the strain associated with having unequal neighbor distances is larger than in lithium. This may partly explain why they favor structures with a single peak in the short distance part of the distribution function—PBP clusters and fcc crystal. So the range of interatomic potentials appears important in determining the relative stability of fivefold PBP and fourfold CSAP structures.

Table VI shows the shape descriptors for the lowest energy isomers at each size. Qualitatively, the shape of our global minima agree with EJM predictions[21,22] at $n=8$, 19, and 20 (quasi-spherical, small ζ), $n=10$, 11, and 12 (prolate), and $n=18$ (oblate), but they disagree at $n=15$–17. Our global minima at $n=13$ and 14 do not have the optimal EJM shapes either, but in both cases the next lowest isomer does. Comparisons are unclear at $n=9$, 13, and 18. Cluster sizes where high-spin ground states occur are $n=11$, 13, and 15–18. Any one of those, except $n=15$, could have a high-spin global minimum ground state according to our LB results.

TABLE VII. Energies (eV) of the most stable Li_n cluster isomer for each *n*, calculated by LB.

n	Atom removal	Atom exchange
6	1.53	−0.01
7	1.54	0.17
8	1.37	0.13
9	1.25	−0.13
10	1.38	0.08
11	1.30	−0.19
12	1.49	0.07
13	1.42	−0.12
14	1.54	0.09
15	1.45	−0.15
16	1.61	0.06
17	1.55	0.09
18	1.45	−0.33
19	1.78	0.23
20	1.50	···

There seems to be a relation between cluster shape and spin state (for a discussion see Ref. 62), and competing factors in achieving low-energy Li_n clusters. With few exceptions ($n=9$ and 11), high-spin ground states occur at sizes where shape deviates from the EJM prediction. A possible rationale is this. Metal clusters generally adopt compact structures. But at certain numbers of electrons, the most compact clusters have an unfavorable shape according to the EJM. This can lead to one of two things: (1) spin alignment in degenerate or near-degenerate orbitals, such as in the 13-atom ICO and 17-atom DTCTP and (2) distortion to a lower symmetry or less compact structure with singlet ground state, such as in all Li_{13} isomers other than ICO and the capped DCSAP 15.1.

IV. SIZE DEPENDENCE OF PROPERTIES

In this section we focus on the lowest energy isomer of each size and look at how cluster properties change with size. Table VII and Fig. 3 show LB energies required for different processes: atom removal, atom exchange, and atomization (cohesive energy):

$$Li_n \rightarrow Li_{n-1} + Li, \tag{5}$$

$$2Li_n \rightarrow Li_{n-1} + Li_{n+1}, \tag{6}$$

$$(1/n)Li_n \rightarrow Li. \tag{7}$$

With our definitions, these energies are positive and larger for the most stable clusters. Cohesive energies are shown in Fig. 3, and our calculated vertical and adiabatic ionization

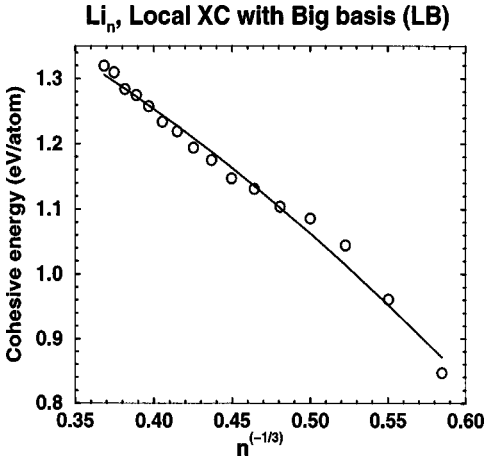

FIG. 3. Calculated cohesive energies of Li_n plotted as a function of $n^{-1/3}$.

potentials are shown in Fig. 4 along with the experimental values of Dugourd *et al.*[40] In calculating adiabatic ionization potentials, we did not do global searches for cation cluster isomers: we only did a local optimization starting from the global minimum geometry of the neutral. The structures we used for clusters with five to eight atoms were found in previous studies: a C_{2v} distorted TBP (Li_5), a D_{4h} flattened octahedron (Li_6), a D_{5h} PBP (Li_7), and a capped CTP (Li_8). The atomization energy of Li_n is simply n times the cohesive energy: it is 4.24 eV for Li_5 and 26.40 eV for Li_{20}. In all calculations we neglected the zero point energies because they are small and cancel out to a large extent.

Atom removal energies point to $n=6$, 7, 16, and 19 as being particularly stable. Atom exchange energies are quite sensitive but they only compare clusters of neighboring sizes: they suggest that $n=7$, 8, and 19 are especially stable. The cohesive energy, E_c, increases gradually as expected. To a first approximation, one expects that $E_c(1/n)$ varies with the relative number of interior, surface, and ''corner'' atoms in a cluster, so that

$$E_c(1/n) \approx E_c(0) + C_1(1/n)^{1/3} + C_2(1/n)^{2/3}. \tag{8}$$

The best fit is obtained with $E_c(0)=1.64$, $C_1=-0.195$, and $C_2=-1.90$. The bulk limit of the fit, $E_c(0)=1.64$ eV/atom, is coincidentally almost equal to the experimental value, 1.63 eV/atom. Comparing actual and fitted cohesive energies gives our preferred way of defining relative stability of clusters. The LB cohesive energies that lie above the fit (full line curve in Fig. 3) are particularly stable; they are $n=7$, 8, 19, and 20. By that same criterion the $n=11-15$ series appears relatively unstable.

The ''magic numbers'' 7, 8, 19, and 20 are interesting in many ways. It is well known that $n=7$, 13, and 19 correspond to closings of atomic shells in the PBP and ICO growth sequence,[10] and here we do find that 7 and 19 are particularly stable. But Li_{19} is *not* a DICO (the DICO is 0.55 eV above the global minimum), and Li_{13} is *not* very stable although it *is* an ICO. The four clusters all have a shape that conforms to the EJM, and the 8- and 20-atom clusters are predicted by EJM to have special stability (closed electronic shells) as we find. This also agrees with previous work.[30] But the 20-atom structures of Ref. 30 have very high energy even though they are fairly compact and have ideal EJM shapes. Curiously, we find two odd-electron species among the four most stable lithium clusters (7, 19). This is surprising because the experimental ionization potentials of Li_n clearly show even–odd oscillations, and closed-shell (even n) silver clusters are systematically more stable than open-shell (odd n) clusters. Arguments based on atomic, electronic, and spin shell closing clearly matter, but they do not fully describe lithium clusters. Stable Li_n clusters tend to have a combination of EJM shape and high mean coordination, and prefer structures with interior atoms. Assuming that is the case also for cluster ions, we expect these closed-shell species to be particularly stable: Li_7^+ in the D_{5h} PBP structure (oblate, 6 electrons), Li_9^+ with D_{4d} CSAP structure (quasi-spherical, 8 electrons; Rao *et al.*[44] also suggested that Li_9^+ is particularly stable), and Li_{19}^- with structure 19.1 (quasi-spherical, 20 electrons).

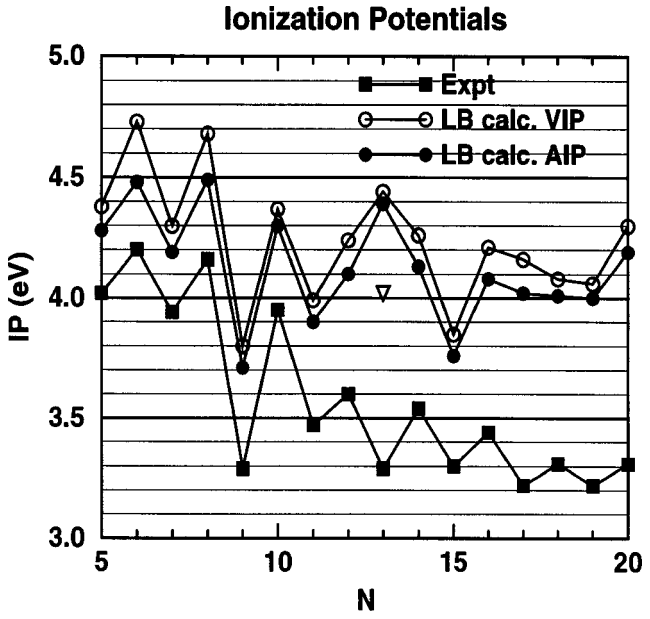

FIG. 4. Vertical and adiabatic ionization potentials obtained by LB calculations, and experimental ionization potentials (Ref. 40).

The LS HOMO-LUMO gaps are shown in Tables III–V. Those calculated by LB (not shown in Tables III–V) are almost equal, they are smaller by an amount ranging between 0.00 and 0.10 eV. In open-shell clusters, we take the HOMO-LUMO gap to be the smallest of the alpha and beta spin gaps. The maximum hardness principle[63] is obeyed in many cases, but not always: global minima have larger HOMO-LUMO gap than any other isomer at $n=6$, 8, 10, 12, 14, 16, and 20. The clusters with the largest gap are 8.1 (1.36 eV) and 20.1 (1.05 eV), both of which are quasi-spherical and correspond to shell closings in the jellium model. Generally, clusters with large HOMO-LUMO gaps have shapes that agree with the EJM, for example, the prolate 10.1 and oblate 14.2.

Our calculated adiabatic ionization potentials (AIP) track the experimental IPs very well for $n<12$, overestimating by a near constant amount (0.25 to 0.4 eV, see Fig. 4). At n

$=12$, our AIP overestimates experiment by 0.5 eV. We calculated two AIP for Li_{13}, one for a quintet state cationic cluster with essentially icosahedral structure and the ICO neutral. The other, shown as a triangle in Fig. 4, was calculated with the energies of the 13.2 cation and the ICO neutral: if we took the energy of the 13.2 neutral instead, our value would go down by 0.05 eV and be more in line with the overall trend. The comparison to experiment suggests that the Li_{13} cluster observed by Dugourd *et al.* was not a high spin state icosahedron; it was more likely a CSAP derived structure. At $n \geqslant 14$, we overestimate experimental IP by 0.45 to 0.9 eV, which is significantly more than the 0.25 to 0.4 eV overestimation at small sizes. There are at least three possible explanations for the discrepancy. First, it could be a size inconsistency error rooted in the LSD exchange correlation. Second, experimental IPs may involve cation structures that are almost fully relaxed, whereas we use the calculated global minimum for the neutral but a local minimum for the cation. If that is true, it implies that large structure changes take place upon ionization for clusters with $n \geqslant 14$. A third explanation is that experiments most likely generate mixtures of isomers. And since experimental IPs are obtained from thresholds, they correspond to the IP of the isomer with lowest IP, not the IP of the most stable isomer as we calculated. The second and third points account for our IPs being larger (not smaller) than the experimental ones.

V. CONCLUDING REMARKS

We did an unbiased global search for minimum energy Li_n cluster structures. One can never be sure to have found the true global minimum, and indeed we have reasons to think we missed it at sizes $n \geqslant 18$. However, we believe that the structures that we found are either global minima, or close to them in energy and in structural features, for the following reasons. First, we do not find any cluster size that is *much* less stable than others. Second, we do find special stability associated with sizes 8 and 20. Finally, the Li_2 dissociation energy and extrapolated bulk cohesive energy are very close to experimental values.

At most sizes there seems to be several competing structures within a small energy range, so experiments would probably sample a mixture of isomers that might interconvert quickly.[26,27,39] But at other sizes (10, 12, 16, 17) our calculated energy separations suggest that lithium clusters could consist of a single quasirigid isomer.

The Li_8 and Li_{20} clusters stand out by their relatively high stability, large HOMO-LUMO gap, and quasi-spherical structure, all of which agree with the EJM. Generally, the EJM helps rationalize the minimum energy structures that we found. But there are many things that it cannot explain, such as the prolate shape of clusters in the range $n=15-17$, and the instability of two T_d symmetry isomers of Li_{20}.

In the size range $8 \leqslant n \leqslant 20$, we find most Li clusters have CSAP-type structures characterized by many interior atoms and a mix of short and long bonds, in agreement with Sung *et al.*[23] Exceptions to this are found at $n=10$, 12, 13, which favor PBP-type structures. The CSAP (centered square antiprism) itself can be viewed as a distorted 9-atom fragment of the bcc crystal structure, so, in a sense, very small lithium clusters look like precursors of solid Li bcc structure. Sufficiently large basis sets are necessary to stabilize the CSAP structures and get reliable relative isomer energies.

Unusual spin states have been suggested for Li_{13},[24] Li_4^-,[29] and small Al clusters.[64] We found that such states could be fairly common among lithium clusters. We find multiplicities higher than singlet or doublet for the ground state or some low energy excited state of Li_n at $n=11$, 13, and 16–18.

ACKNOWLEDGMENTS

We thank Dr. Gary Leach and Dr. Robert Hudgins for discussions about experimental measurements of cluster ionization potentials. This work was supported by the Natural Sciences and Engineering Research Council of Canada and by Research Corporation.

[1] J. Jortner, in *Physics and Chemistry of Finite Systems: From Clusters to Crystals* (Kluwer, Netherlands, 1992), Vol. 1, pp. 1–17.
[2] M. D. Morse, M. E. Geusic, J. R. Heath, and R. E. Smalley, J. Chem. Phys. **83**, 2293 (1985).
[3] A. J. Cox, J. G. Louderback, and L. A. Bloomfield, Phys. Rev. Lett. **71**, 923 (1993).
[4] S. J. Riley, Ber. Bunsenges. Phys. Chem. **96**, 1104 (1992).
[5] M. B. Knickelbein, Annu. Rev. Phys. Chem. **50**, 79 (1999).
[6] O. Echt, K. Sattler, and E. Recknagel, Phys. Rev. Lett. **47**, 1121 (1981).
[7] W. Miehle, O. Kandler, T. Leisner, and O. Echt, J. Chem. Phys. **91**, 5940 (1989).
[8] J. Farges, M. F. de Feraudy, B. Raoult, and G. Torchet, Adv. Chem. Phys. **70** (part 2), 45 (1988).
[9] M. R. Hoare, Adv. Chem. Phys. **40**, 49 (1979); C. J. Tsai and K. D. Jordan, J. Phys. Chem. **97**, 1127 (1993).
[10] T. P. Martin, Phys. Rep. **273**, 199 (1996), and references therein.
[11] P. W. Fowler and D. E. Manolopoulos, *An Atlas of Fullerenes*, International Series of Monographs on Chemistry No. 30 (Clarendon, Oxford, 1995).
[12] S. Li, R. J. Van Zee, W. Weltner, Jr., and K. Raghavachari, Chem. Phys. Lett. **243**, 275 (1995).
[13] I. Rata, A. A. Shvartsburg, M. Horoi, T. Frauenheim, K. W. M. Siu, and K. A. Jackson, Phys. Rev. Lett. **85**, 546 (2000).
[14] E. C. Honea, A. Ogura, D. R. Peale, C. Félix, C. A. Murray, K. Raghavachari, W. O. Sprenger, M. F. Jarrold, and W. L. Brown, J. Chem. Phys. **110**, 12161 (1999).
[15] H. Kietzmann, J. Morenzin, P. S. Bechthold *et al.*, Phys. Rev. Lett. **77**, 4528 (1996).
[16] E. K. Parks, L. Zhu, J. Ho, and S. J. Riley, J. Chem. Phys. **100**, 7206 (1994).
[17] J. Akola, M. Manninen, H. Häkkinen, U. Landmann, X. Li, and L.-S. Wang, Phys. Rev. B **60**, R11297 (1999).
[18] B. J. Winter, E. K. Parks, and S. J. Riley, J. Chem. Phys. **94**, 8618 (1991).
[19] T. D. Klots, B. J. Winter, E. K. Parks, and S. J. Riley, J. Chem. Phys. **92**, 2110 (1990).
[20] E. K. Parks, T. D. Klots, B. J. Winter, and S. J. Riley, J. Chem. Phys. **99**, 5831 (1993).
[21] W. A. DeHeer, Rev. Mod. Phys. **65**, 611 (1993); M. Brack, *ibid.* **65**, 677 (1993) and references therein.
[22] C. Yannouleas and U. Landman, Phys. Rev. B **51**, 1902 (1995).
[23] M.-W. Sung, R. Kawai, and J. H. Weare, Phys. Rev. Lett. **73**, 3552 (1994).
[24] G. Gardet, F. Rogemond, and H. Chermette, J. Chem. Phys. **105**, 9933 (1996).
[25] R. Kawai, J. F. Tombrello, and J. H. Weare, Phys. Rev. A **49**, 4236 (1994); R. Kawai, M. W. Sung, and J. H. Weare, in *Physics and Chemistry of Finite Systems: From Clusters to Crystals*, NATO ASI Series (Kluwer Academic, Amsterdam, 1992), Vol. 1, pp. 441–446.
[26] R. Rousseau and D. Marx, Phys. Rev. Lett. **80**, 2574 (1998).
[27] R. Rousseau and D. Marx, J. Chem. Phys. **111**, 5091 (1999).
[28] H. W. Sarkas, S. T. Arnold, J. H. Hendricks, and K. H. Bowen, J. Chem. Phys. **102**, 2653 (1995).

[29] B. K. Rao, P. Jena, and A. K. Ray, Phys. Rev. Lett. **76**, 2878 (1996).
[30] J. Koutecký, V. Bonačić-Koutecký, I. Boustani, P. Fantucci, and W. Pewestorf, in *Large Finite Systems*, edited by J. Jortner and B. Pullman (Reidel, Dordrecht, 1987), pp. 303–317.
[31] V. Bonačić-Koutecký, J. Pittner, C. Fuchs, P. Fantucci, and J. Koutecký, in *Physics and Chemistry of Finite Systems: From Clusters to Crystals*, NATO ASI Series (Kluwer Academic, Dordrecht, 1992), Vol. 1.
[32] J. Koutecký, I. Boustani, and V. Bonačić-Koutecký, Int. J. Quantum Chem. **38**, 149 (1990).
[33] J. Cheng, M.Sc. thesis, York University, 2002; J. Cheng and R. Fournier (unpublished).
[34] R. Rousseau and D. Marx, Phys. Rev. A **56**, 617 (1997).
[35] G. Gardet, F. Rogemond, and H. Chermette, Theor. Chim. Acta **91**, 249 (1995).
[36] P. Dugourd, J. Blanc, V. Bonačić-Koutecký, M. Broyer, J. Chevaleyre, J. Koutecký, J. Pittner, J. P. Wolf, and L. Wöste, Phys. Rev. Lett. **67**, 2638 (1991).
[37] J. Blanc, V. Bonačić-Koutecký, M. Broyer, J. Chevaleyre, P. Dugourd, J. Koutecký, C. Scheuch, J. P. Wolf, and L. Wöste, J. Chem. Phys. **96**, 1793 (1992).
[38] J. M. Pacheco and J. L. Martins, J. Chem. Phys. **106**, 6039 (1997).
[39] D. Reichardt, V. Bonačić-Koutecký, P. Fantucci, and J. Jellinek, Chem. Phys. Lett. **279**, 129 (1997).
[40] P. Dugourd, D. Rayane, P. Labastie, B. Vezin, J. Chevaleyre, and M. Broyer, Chem. Phys. Lett. **197**, 433 (1992).
[41] C. Yannouleas and U. Landman, J. Chem. Phys. **107**, 1032 (1997); G. Gardet, F. Rogemond, and H. Chermette, *ibid.* **107**, 1034 (1997).
[42] S. Ishii, K. Ohno, Y. Kawazoe, and S. G. Louie, Phys. Rev. B **65**, 245109 (2002).
[43] C. Yannouleas, U. Landman, C. Bréchignac, P. Cahuzac, B. Concina, and J. Leygnier, Phys. Rev. Lett. **89**, 173403 (2002).
[44] B. K. Rao, P. Jena, M. Manninen, and R. M. Nieminen, Phys. Rev. Lett. **58**, 1188 (1987).
[45] R. Rousseau and D. Marx, Chem. Eur. J. **6**, 2982 (2000).
[46] A. St-Amant and D. R. Salahub, Chem. Phys. Lett. **169**, 387 (1990); A. St-Amant, Ph.D. thesis, University of Montreal, 1992; deMon-KS version 3.2, M. E. Casida, C. Daul, A. Goursot, A. Koester, L. G. M. Pettersson, E. Proynov, A. St-Amant, and D. R. Salahub (principal authors), and S. Chretien, H. Duarte, N. Godbout *et al.* (contributing authors), deMon Software, 1998.
[47] S. H. Vosko, L. Wilk, and M. Nusair, Can. J. Phys. **58**, 1200 (1980).
[48] A. D. Becke, Phys. Rev. A **38**, 3098 (1988).
[49] J. P. Perdew, Phys. Rev. B **33**, 8822 (1986).
[50] Basis sets were obtained from the Extensible Computational Chemistry Environment Basis Set Database, Version 10/29/02, as developed and distributed by the Molecular Science Computing Facility, Environmental and Molecular Sciences Laboratory which is part of the Pacific Northwest Laboratory, P.O. Box 999, Richland, Washington 99352, and funded by the U.S. Department of Energy. The Pacific Northwest Laboratory is a multi-program laboratory operated by Battelle Memorial Institue for the U.S. Department of Energy under Contract No. DE-AC06-76RLO 1830. Contact David Feller or Karen Schuchardt for further information.
[51] T. H. Dunning, Jr., J. Chem. Phys. **90**, 1007 (1989).
[52] J. P. Perdew and Y. Wang, Phys. Rev. B **46**, 12947 (1992); E. I. Proynov, A. Vela, and D. R. Salahub, Phys. Rev. A **50**, 3766 (1994); E. I. Proynov, E. Ruiz, A. Vela, and D. R. Salahub, Int. J. Quant. Chem. Symp. **29**, 61 (1995).
[53] J. P. Perdew, S. Kurth, A. Zupan, and P. Blaha, Phys. Rev. Lett. **82**, 2544 (1999).
[54] S. Yanagisawa, T. Tsuneda, and K. Hirao, J. Chem. Phys. **112**, 545 (2000).
[55] C. J. Barden, J. C. Rienstra-Kiracofe, and H. F. Schaefer III, J. Chem. Phys. **113**, 690 (2000).
[56] K. P. Huber and G. Herzberg, *Molecular Spectra and Molecular Structure, Vol. IV, Constants of Diatomic Molecules* (Van Nostrand, Toronto, 1979).
[57] The Cartesian coordinates of the clusters are available upon request to R.F.
[58] D. A. McQuarrie, *Statistical Mechanics* (Harper & Row, New York, 1976), p. 137, Eq. 8–33.
[59] R. Fournier, J. Chem. Phys. **115**, 2165 (2001).
[60] Our best structure is very close to C_{2v}, but it is actually C_s likely because of numerical errors and imperfect convergence in the geometry optimization.
[61] J. P. K. Doye and D. J. Wales, Science **271**, 484 (1996); J. P. K. Doye, D. J. Wales, and R. S. Berry, J. Chem. Phys. **103**, 4234 (1995).
[62] B. K. Rao, P. Jena, and M. Manninen, Phys. Rev. B **32**, 477 (1985).
[63] M. Solá and A. Toro-Labbé, J. Phys. Chem. A **103**, 8847 (1999); P. Perez and A. Toro-Labbé, *ibid.* **104**, 1557 (2000).
[64] B. K. Rao and P. Jena, J. Chem. Phys. **111**, 1890 (1999).